PRIFYSGOL ABERYSTWYTH UNIVERSITY

Aberystwyth University

High temperature photoelectron emission and surface photovoltage in semiconducting diamond

Williams, G. T.; Cooil, S. P.; Roberts, O. R.; Evans, S.; Langstaff, D. P.; Evans, D. A.

Published in:
Applied Physics Letters

DOI:
10.1063/1.4893274

Publication date:
2014

Citation for published version (APA):
Williams, G. T., Cooil, S. P., Roberts, O. R., Evans, S., Langstaff, D. P., & Evans, D. A. (2014). High temperature photoelectron emission and surface photovoltage in semiconducting diamond. *Applied Physics Letters*, *105*(6), Article 061602. https://doi.org/10.1063/1.4893274

Document License
CC BY

General rights
Copyright and moral rights for the publications made accessible in the Aberystwyth Research Portal (the Institutional Repository) are retained by the authors and/or other copyright owners and it is a condition of accessing publications that users recognise and abide by the legal requirements associated with these rights.

• Users may download and print one copy of any publication from the Aberystwyth Research Portal for the purpose of private study or research.
• You may not further distribute the material or use it for any profit-making activity or commercial gain
• You may freely distribute the URL identifying the publication in the Aberystwyth Research Portal

Take down policy
If you believe that this document breaches copyright please contact us providing details, and we will remove access to the work immediately and investigate your claim.

tel: +44 1970 62 2400
email: is@aber.ac.uk

Download date: 15. Jun. 2024

High temperature photoelectron emission and surface photovoltage in semiconducting diamond

G. T. Williams, S. P. Cooil, O. R. Roberts, S. Evans, D. P. Langstaff, and D. A. Evans

Citation: Applied Physics Letters **105**, 061602 (2014); doi: 10.1063/1.4893274
View online: http://dx.doi.org/10.1063/1.4893274
View Table of Contents: http://scitation.aip.org/content/aip/journal/apl/105/6?ver=pdfcov
Published by the AIP Publishing

Articles you may be interested in

High-reliability passivation of hydrogen-terminated diamond surface by atomic layer deposition of Al2O3
J. Appl. Phys. **115**, 223711 (2014); 10.1063/1.4881524

Work function and electron affinity of the fluorine-terminated (100) diamond surface
Appl. Phys. Lett. **102**, 091604 (2013); 10.1063/1.4793999

Photoelectron emission properties of hydrogen terminated intrinsic diamond
J. Appl. Phys. **99**, 086102 (2006); 10.1063/1.2188070

In situ photovoltage measurements using femtosecond pump-probe photoelectron spectroscopy and its application to metal– Hf O 2 – Si structures
J. Vac. Sci. Technol. A **23**, 1698 (2005); 10.1116/1.2083909

High-resolution synchrotron-radiation photoemission characterization for atomically-controlled SrTiO 3 (001) substrate surfaces subjected to various surface treatments
J. Appl. Phys. **96**, 7183 (2004); 10.1063/1.1814175

AIP | Journal of Applied Physics

Journal of Applied Physics is pleased to announce André Anders as its new Editor-in-Chief

This article is copyrighted as indicated in the article. Reuse of AIP content is subject to the terms at: http://scitation.aip.org/termsconditions. Downloaded to IP: 144.124.48.127 On: Tue, 26 Aug 2014 09:12:23

High temperature photoelectron emission and surface photovoltage in semiconducting diamond

G. T. Williams,[a] S. P. Cooil, O. R. Roberts,[b] S. Evans, D. P. Langstaff, and D. A. Evans[c]
Department of Physics, Aberystwyth University, Aberystwyth, Ceredigion SY23 3BZ, United Kingdom

(Received 18 July 2014; accepted 2 August 2014; published online 13 August 2014)

A non-equilibrium photovoltage is generated in semiconducting diamond at above-ambient temperatures during x-ray and UV illumination that is sensitive to surface conductivity. The H-termination of a moderately doped p-type diamond (111) surface sustains a surface photovoltage up to 700 K, while the clean (2×1) reconstructed surface is not as severely affected. The flat-band C 1s binding energy is determined from 300 K measurement to be 283.87 eV. The true value for the H-terminated surface, determined from high temperature measurement, is (285.2 ± 0.1) eV, corresponding to a valence band maximum lying 1.6 eV below the Fermi level. This is similar to that of the reconstructed (2×1) surface, although this surface shows a wider spread of binding energy between 285.2 and 285.4 eV. Photovoltage quantification and correction are enabled by real-time photoelectron spectroscopy applied during annealing cycles between 300 K and 1200 K. A model is presented that accounts for the measured surface photovoltage in terms of a temperature-dependent resistance. A large, high-temperature photovoltage that is sensitive to surface conductivity and photon flux suggests a new way to use moderately B-doped diamond in voltage-based sensing devices. © *2014 Author(s). All article content, except where otherwise noted, is licensed under a Creative Commons Attribution 3.0 Unported License*. [http://dx.doi.org/10.1063/1.4893274]

The electrical conductivity of semiconducting diamond can be controlled by bulk and surface doping[1,2] to enable device applications such as diodes,[3] transistors,[4] and radiation sensors,[5] in particular, in extreme environments (high temperature, high radiation).[6] Electronic quality p-type material[7] can be semiconducting, metallic or superconducting, according to the B concentration and temperature.[2] The electronic nature of the surface region is also an important consideration in realizing single-photon, nanoscale quantum devices.[8] In many applications, the crucial parameter is the Fermi level position relative to the band edges within the bulk and at the surface or interface. For moderately doped diamond, a range of values has been reported for the surface Fermi level even for the simplest terminations (O, H, and C) of low index faces. For example, a difference of 0.74 eV has been reported between H-terminated and adsorbate-free diamond (111) surfaces.[9] For metal contacts to diamond surfaces, there is a considerable spread in Fermi level position relative to the band edge, clustered around the charge neutrality level in the lower half of the band gap.[10] Although this can be attributed to surface preparation and metal-induced states, the measurement process, in particular, using photoelectron-based methods, must also be considered.

Here, we show, using real-time and temperature-programmed photoelectron spectroscopy, that room temperature measurements on moderately B-doped diamond are severely affected by a photon-induced surface voltage and there is little difference in the true surface Fermi level position of the H-terminated and adsorbate-free reconstructed surface of (111) diamond, although there is a large difference in surface conductivity. The surface photovoltage (SPV), inferred from the core level binding energy, persists for several hundred degrees above room temperature.

Departure from charge equilibrium is known to be an issue in the correct interpretation of photoelectron emission spectra for wide-gap semiconductors, especially at low temperatures.[11–13] The creation of charge-pairs within the depletion region leads to charge accumulation at the surface, generating a photovoltage that flattens the bands. Ignoring this effect leads to incorrect binding energies at lower (higher) energy for p-type (n-type) materials.

A custom-built ultrahigh vacuum (UHV) system, consisting of connected analysis and processing chambers, was used for *in-situ* preparation of surfaces and real-time photoelectron spectroscopy. Processing chambers enable *in-situ* hydrogenation and oxidation, point-probe electrical measurement, and metal evaporation. The analysis chamber provides indirect heating, Low Energy Electron Diffraction (LEED), X-ray Photoelectron Spectroscopy (XPS), and Ultra-violet Photoelectron Spectroscopy (UPS). Real-time monitoring of surface processes, enabled by parallel electron detection (SPECS Phoibos 100), provides accurate peak intensities and energy positions, calibrated relative to the Cu $2p_{3/2}$ and Au $4f_{7/2}$ core-levels of a clean calibration sample.

The diamond sample (type IIb (B concentration $\sim 10^{21}$ m^3) of dimensions $8.7 \times 5.0 \times 1\,mm^3$ with a [111] orientation) was prepared by polishing, chemical oxidation and *in-situ* annealing and hydrogenation. A metallic Au back contact ensured good electrical contact with the sample holder. The composition and (1×1) bulk-terminated structure of the H-terminated surface were confirmed by XPS and LEED.

A typical C 1s core-level spectrum for the oxygen-free, (1×1):H surface, measured at room temperature, is shown

[a]Current address: Element Six Global Innovation Centre, Didcot, Oxon OX11 0QR, United Kingdom.
[b]Current address: National Library of Wales, Aberystwyth, Ceredigion SY23 3BU, United Kingdom.
[c]Author to whom correspondence should be addressed. Electronic mail: a.evans@aber.ac.uk

 © Author(s) 2014

This article is copyrighted as indicated in the article. Reuse of AIP content is subject to the terms at: http://scitation.aip.org/termsconditions. Downloaded to IP: 144.124.48.127 On: Tue, 26 Aug 2014 09:12:23

in Figure 1(a), and the corresponding spectrum for the adsorbate-free (2×1) reconstructed surface, formed by *in-vacuo* annealing to 1200 K is shown in Figure 1(b). Curve fitting (solid lines in Figures 1(a) and 1(b)) yields a single dominant C-C peak (bulk diamond) with a small C-H peak (surface) at higher binding energy for the (1×1):H surface and a small surface sp^2 carbon peak at lower binding energy for the (2×1) surface. The binding energy of the main C 1s peak (284.0 eV) for the (1×1):H surface is lower than that reported by Pate (284.3 eV)[14] and is significantly lower than that reported by Cui *et al.* (284.8 eV).[9] This value was however found to be process dependent, showing variation from sample to sample. Our lowest measured value was 283.87 eV and this is taken as the flat-band binding energy for our diamond (111) sample. The binding energy of the main core level component for the (2×1) surface (285.1 eV) is larger than that measured at room temperature by Pate (284.8 eV)[14] but close to that measured by Cui *et al.*[9] (285.0 eV). Cui *et al.* also report a higher binding energy (2×1) surface (285.9 eV) when the diamond is heated to 1400 K.

Interestingly, the binding energy of the C 1s core level for the (1×1):H surface was found to be markedly different when *measured* at different temperatures, while there was little change in the binding energy for the (2×1) surface. The temperature dependence of the C 1s core level during heating cycles between 300 K and 960 K was determined by continuous recording of 4 s snapshots as shown in Figures 1(c) and 1(d).

The (2×1) surface (Figure 1(d)) shows little binding energy change with temperature, while the (1×1):H surface (Figure 1(c)) shows a large, reversible shift during this cycle. At high temperature, the binding energies for both surfaces are similar. To quantify the shift, the binding energy was extracted from the real-time data by curve fitting each of the C 1s snapshot spectra. In Figure 2, the binding energy variation during three annealing cycles is presented along with selected LEED patterns, recorded at ambient and elevated temperatures.

In the first heating cycle (Figure 2(a)), the C 1s binding energy for the (1×1):H surface increased rapidly up to 700 K (region 1). Between 700 K and 960 K (region 2), the binding energy remained constant at 285.2 eV. During cooling (regions 3 and 4), the 1.3 eV binding energy shift was completely reversed.

During a second, 1200 K annealing cycle (Figure 2(b)), the C 1s binding energy reversed its direction of change at 1000 K and at 1110 K. There was no return to the original binding energy when this surface was cooled to 300 K. The temperature of 1000 K corresponds to the onset of the (2×1) reconstruction, in agreement with Cui *et al.*[9] During the final 960 K heating cycle of the (2×1) surface (Figure 2(c)), the binding energy showed only a small (0.07 eV) reversible shift.

The reversible shift observed for the (1×1):H surface could be due to a chemical change, for example, a gradual desorption of hydrogen or a change in the C-H and C-C bonding at the surface. However, this would be expected to result in an irreversible binding energy shift as the surface states responsible for Fermi level pinning are modified in energy and/or density. To account for the observed reversible shift, this chemical change would need to be reversed on cooling to 300 K, for example, by a re-adsorption of hydrogen.

The H-terminated surface (Figure 2(a)) has the characteristic 1×1 LEED pattern of the sp^3-bonded surface, while the reconstructed surface (Figure 2(c)) has a three-domain 2×1 LEED pattern that results from the formation of π-bonded chains.[15] The LEED pattern for the intermediate surface, measured at 740 K (Figure 2(b)) has a 1×1 periodicity as for the H-terminated surface. The corresponding C 1s core level, recorded at 740 K, is similar in lineshape to the 300 K spectrum apart from a smaller C-H component, but with a

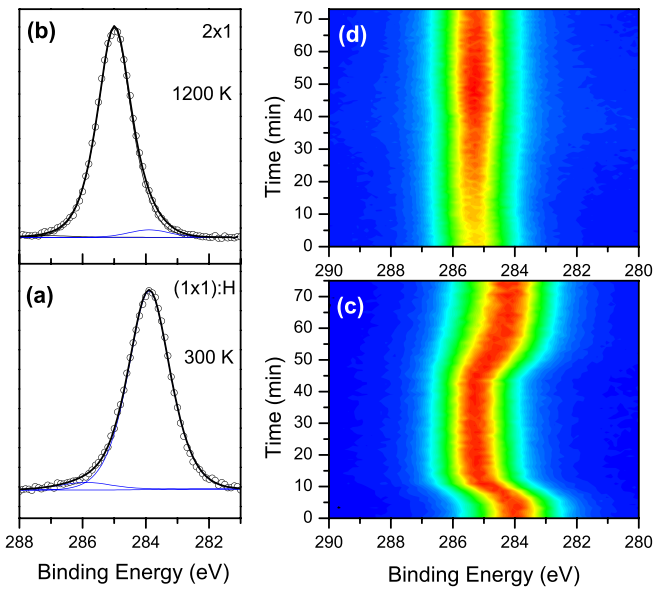

FIG. 1. C 1s core-level photoelectron spectra of the (1×1):H diamond (111) surface measured at room temperature (a) and of the adsorbate-free (2×1) reconstructed surface obtained by annealing to 1200 K (b). Both spectra were measured at room temperature; the open symbols represent the data and the solid lines the fit components. Real-time sequences of C 1s spectra during 300 K–960 K–300 K cycles are shown for the H-terminated surface (c) and for the (2×1) reconstructed surface (d).

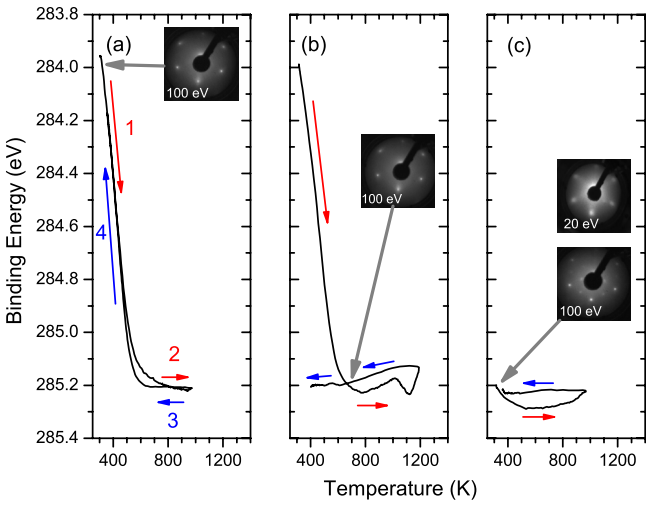

FIG. 2. C1s binding energy changes for the diamond (111) surface during successive annealing cycles from 300 K to (a) 960 K, (b) 1200 K, and (c) 960 K. The 1.26 eV shift is reversible in (a); irreversible in (b) and absent in (c). LEED patterns are shown in (a) at 300 K, in (b) at 740 K, and in (c) at 300 K.

This article is copyrighted as indicated in the article. Reuse of AIP content is subject to the terms at: http://scitation.aip.org/termsconditions. Downloaded to IP: 144.124.48.127 On: Tue, 26 Aug 2014 09:12:23

binding energy close to the (2×1) surface. LEED and XPS measurements therefore suggest that the surface is not reconstructed at temperatures below 1000 K, even though the C 1s binding energy is strongly temperature-dependent.

An alternative, physical explanation is thus more likely, based on non-equilibrium charging during photoexcitation within the diamond. Charging due to the photoemitted current alone can be discounted as this would result in a positively charged surface and a reduction in binding energy. The observed *increase* in binding energy requires a negatively charged surface, as generated by charge separation within the depletion region of a p-type semiconductor under irradiation with above band-gap light.

The reversible shift with temperature of the (1×1):H surface is characteristic of SPV generation, although it is unusual to observe such an effect at high temperatures. The absence of a SPV for the (2×1) surface suggests that an additional conduction path is present, due to a larger surface conductivity. This is consistent with electronic band structure calculations that predict a metallic nature for the reconstructed surface due to surface bands that intersect the Fermi level.[16] Low electron energy LEED patterns recorded at 20 eV showing the second order spots (Figure 2(c)) reflects the high surface conductivity of this surface. At higher temperatures, it has been reported that the conductivity of the (111) surfaces is due to termination by a graphitic[9] or graphene[16,17] layer. The SPV accounts for the spread in C 1s binding energy reported for the (1×1):H surface including that measured by Cui *et al.*,[9] who studied a diamond with a higher B concentration. For diamonds with very high B-concentration ($\sim 10^{26}\,m^{-3}$), we have observed no shift in the C 1s binding energy during temperature cycling. The true value for the C 1s binding energy for the (1×1):H surface was found to lie in the range (285.2 ± 0.1) eV and the C 1s binding energy for the (2×1) surface was found to lie at the same value $((285.2 \pm 0.2)$ eV) but with a larger spread from sample to sample. The highest measured binding energy for the latter (285.42 eV) was obtained for a high temperature surface that showed the narrowest linewidth, the sharpest second order LEED spots and a zero energy shift with temperature. This is close to the highest temperature surface measured by Cui *et al.* for their graphitic surface.[9]

The room temperature SPV also affected ultraviolet (He I) photoemission measurements in the same environment as shown in Figure 3(a). The temperature shift in the photoelectron spectrum mirrors that of the XPS data although the magnitude is different for the two excitation sources. UPS data can also therefore yield incorrect values for the (1×1):H surface band bending at room temperature.

In Figure 3(b), the dependence of the C 1s binding energy on incident x-ray flux is shown for the (1×1):H (open symbols) and (2×1) (closed symbols) surfaces. No change was found for the (2×1) surface, while a shift of 0.28 eV was measured for the (1×1):H surface when the x-ray power was reduced from 300 W to 3 W. This confirms the presence of a strong SPV for the (1×1):H surface but not for the more conductive (2×1) surface.

Having established the SPV mechanism, a model has been derived to account for the reversible temperature dependence observed in the real-time photoemission data.

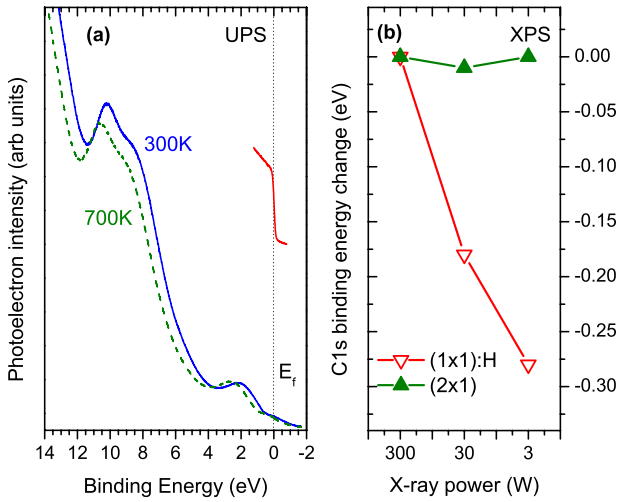

FIG. 3. (a) UPS valence band photoelectron spectra for the (1×1):H diamond (111) surface, measured using He I radiation. The binding energy is referenced to a metal Fermi level (red line). Spectra recorded at 300 K (solid line) and at 700 K (dashed line) are similar in lineshape but shifted in binding energy. (b) The C1s binding energy position for the (1×1):H surface (open symbols) shows a strong x-ray power dependence, whereas that for the (2×1) surface (closed symbols) does not.

When above band-gap radiation is incident on the diamond, the electron-hole generation depends on the photon flux (Φ_{ph}), the number of pairs generated per photon (η), the photon attenuation length (λ_{ph}) and the width of the depletion region (d). The resultant internal current density is given by

$$j_i = q\eta\Phi_{ph}\left(1 - e^{-\frac{d}{\lambda_{ph}}}\right). \tag{1}$$

The current density is greatest for high photon energy and flux and for moderately doped semiconductors where the depletion width is comparable to or greater than the attenuation length of the photons. The equilibrium depletion width for a moderately doped diamond ($10^{20}\,m^{-3}$) with a Schottky barrier of 1.3 V is calculated to be around 1 μm. This value is similar to the photon attenuation length ($\lambda_{\pi\eta}$) for Mg Kα x-rays in low Z materials and therefore Eq. (1) can be simplified to provide an expression (Eq. (2)) for the internal current, I_i in terms of band-bending, V_{bb}, area of irradiation, A, dielectric constant, ε_r, and acceptor concentration, N_A,

$$I_i = \frac{0.63q\eta A\Phi_{ph}}{\lambda}\left(\frac{2\varepsilon_0\varepsilon_r V_{bb}}{qN_A}\right)^{\frac{1}{2}}. \tag{2}$$

The flux density Φ_{ph} was estimated as 10^9 photons $s^{-1}\,mm^{-2}$ and the acceptor concentration was assumed equal to the B concentration ($N_A = 10^{21}\,m^{-3}$) for full ionization at high temperature. The acceptor concentration reduces to $10^{19}\,m^{-3}$ at 300 K, reflecting the temperature dependence of the hole mobility.[18] The value of η is given by the electron–hole production per photon within the depletion region and is approximated by $h\nu/E_G = 230$. The flat-band C 1s core-level binding energy is taken as 283.9 eV, corresponding to a maximum band bending, $V_{bb} = 1.26$ V. Taking the x-ray penetration length $\lambda = 1\,\mu m$ ($\sim$d), the maximum internal current generated at equilibrium is 3×10^{-6} A.

During irradiation of such a semiconductor by x-rays, a surface photovoltage is generated if the conductivity is

This article is copyrighted as indicated in the article. Reuse of AIP content is subject to the terms at: http://scitation.aip.org/termsconditions. Downloaded to IP: 144.124.48.127 On: Tue, 26 Aug 2014 09:12:23

insufficient for the internal current I_i to be compensated by a restoring current. In the Hecht model,[12] the semiconductor is considered as an ideal Schottky diode under forward bias. The restoring current results from thermionic emission across the potential barrier, given by an expression similar to that used to analyze I–V characteristics for Schottky diodes under low forward bias.[19]

The observed surface photovoltage effect in photoemission experiments on III–V semiconductors[11] was attributed to a low restoring current for large barriers at reduced temperatures. This model enabled the true surface band-bending for semiconductors such as GaAs and GaP to be determined.[11] Further refinements included the effect of a shunt resistance, established for example, during the growth of thin metal films on the surface.[20]

For larger gap materials, such as diamond[21] and GaN,[13] it has been shown that the surface photovoltage can persist up to room temperature. However, for GaN, Long and Bermudez[13] were unable to account for their measurements at using an SPV mechanism based on existing models.

Our model uses a mechanism based on the temperature dependence of the resistance, carrier concentration, depletion width, and internal photocurrent to quantitatively account for the measured SPV. An iterative numerical model was generated using Eq. (3) to reproduce the observed shift in C 1s binding energy as shown in Figure 4. The experimental data are represented by the open symbols and the model by the cross symbols.

$$V_{SPV} = \frac{0.63q\eta A\Phi_{ph}}{\lambda}\left(\frac{2\varepsilon_0\varepsilon_r}{qN_A}\right)^{\frac{1}{2}} V_{bb}^{\frac{1}{2}} R(T). \tag{3}$$

The temperature dependence of the diamond resistance (R(T)) was determined experimentally from point-contact I-V-T measurements using a gold probe in the same experimental environment as the photoemission measurements. Measured values varied from 500 kΩ at 300 K to 3 kΩ at 900 K, as shown in the inset of Figure 4. The solid line shows the best fit to the data assuming an Arrhenius relationship, with an activation energy of 0.18 eV.

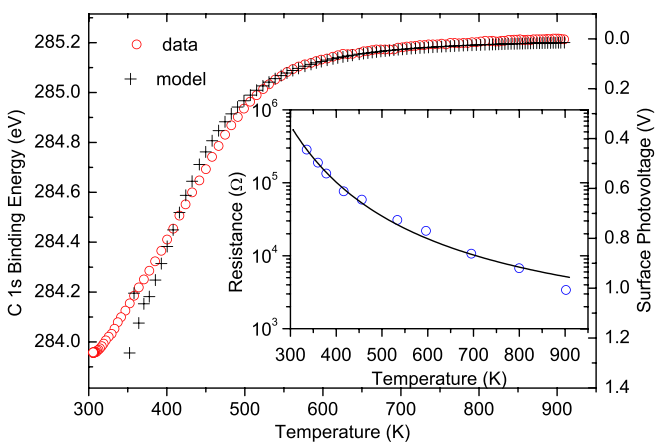

FIG. 4. Model of the temperature dependence of the binding energy (solid line) in comparison with changes in the measured C1s core level binding energy (open symbols). Inset is the measured resistance change with temperature (open symbols) determined from *in-situ* IV data for a Au point probe on the (1 × 1):H diamond surface.

At high temperature, the resistance is low and the system is at equilibrium, with negligible SPV. The model reproduces the observed onset of SPV as the temperature is reduced; it becomes unstable as the band-bending approaches zero and terminates at around 350 K. The divergence between experiment and model at lower temperatures is due to other contact resistances that are not explicitly considered in this model.

In summary, we have identified an above-ambient SPV for moderately doped semiconducting diamond that leads to erroneous values of band-bending for the (1 × 1):H diamond (111) surface at room temperature. The true Fermi level position for this surface is similar to the (2 × 1) reconstructed surface. However, the surface conductivity in vacuum is different, leading to SPV generation only for the (1 × 1):H surface. The measured temperature change of the C 1s binding energy for the (1 × 1):H surface in real-time photoemission experiments has been modeled using the temperature-dependence of the resistance. The above-ambient, non-equilibrium voltage at the (1 × 1):H diamond surface is sensitive to photon flux and surface conductivity and therefore offers new applications of semiconducting diamond as voltage-based detector of above band-gap radiation and as a sensor for adsorbates that change the surface conductivity.

This work was funded by the EPSRC (EP/G068216/1) and was performed within the Centre for Advanced Functional Materials and Devices, a HEFCW-funded Research and Enterprise Partnership; G.T.W. acknowledges an Aberystwyth University Postgraduate Research Scholarship.

[1]P. Strobel, M. Riedel, J. Ristein, and L. Ley, Nature **430**(6998), 439–441 (2004).
[2]T. Yokoya, T. Nakamura, T. Matsushita, T. Muro, Y. Takano, M. Nagao, T. Takenouchi, H. Kawarada, and T. Oguchi, Nature **438**(7068), 647–650 (2005).
[3]D. J. Twitchen, A. J. Whitehead, S. E. Coe, J. Isberg, J. Hammersberg, T. Wikstrom, and E. Johansson, IEEE Trans. Electron Devices **51**(5), 826–828 (2004).
[4]S. P. Lansley, H. J. Looi, Y. Y. Wang, M. D. Whitfield, and R. B. Jackman, Appl. Phys. Lett. **74**(4), 615–617 (1999).
[5]H. Kagan, Nucl. Instrum. Methods Phys. Res., Sect. A **541**(1–2), 221 (2005).
[6]C. J. H. Wort and R. S. Balmer, Mater. Today **11**(1–2), 22–28 (2008).
[7]J. Isberg, J. Hammersberg, E. Johansson, T. Wikstrom, D. J. Twitchen, A. J. Whitehead, S. E. Coe, and G. A. Scarsbrook, Science **297**(5587), 1670–1672 (2002).
[8]T. M. Babinec, B. J. M. Hausmann, M. Khan, Y. Zhang, J. R. Maze, P. R. Hemmer, and M. Loncar, Nat. Nanotechnol. **5**(3), 195–199 (2010).
[9]J. B. Cui, J. Ristein, and L. Ley, Phys. Rev. B **59**(8), 5847–5856 (1999).
[10]D. A. Evans, O. R. Roberts, G. T. Williams, A. R. Vearey-Roberts, F. Bain, S. Evans, D. P. Langstaff, and D. J. Twitchen, J. Phys.: Condens. Matter **21**(36), 364223 (2009).
[11]M. Alonso, R. Cimino, and K. Horn, Phys. Rev. Lett. **64**(16), 1947–1950 (1990).
[12]M. H. Hecht, J. Vac. Sci. Technol., B **8**(4), 1018–1024 (1990).
[13]J. P. Long and V. M. Bermudez, Phys. Rev. B **66**(12), 121308 (2002).
[14]B. B. Pate, Surf. Sci. **165**(1), 83–142 (1986).
[15]K. C. Pandey, Phys. Rev. B **25**(6), 4338–4341 (1982).
[16]W. Hu, Z. Li, and J. Yang, J. Chem. Phys. **138**(5), 054701 (2013).
[17]T. Norio, F. Makoto, M. Toshiharu, T. Daisuke, Y. Satoshi, and I. Takao, Jpn. J. Appl. Phys., Part 1 **52**(11R), 110121 (2013).
[18]J. Pernot, P. N. Volpe, F. Omnès, P. Muret, V. Mortet, K. Haenen, and T. Teraji, Phys. Rev. B **81**(20), 205203 (2010).
[19]E. H. Rhoderick and R. H. Williams, *Metal-Semiconductor Contacts* (Clarendon Press, Oxford, 1988).
[20]D. A. Evans, T. P. Chen, T. Chasse, and K. Horn, Appl. Surf. Sci. **56–8**, 233–241 (1992).
[21]C. Bandis and B. B. Pate, Surf. Sci. **345**(1–2), L23–L27 (1996).

This article is copyrighted as indicated in the article. Reuse of AIP content is subject to the terms at: http://scitation.aip.org/termsconditions. Downloaded to IP: 144.124.48.127 On: Tue, 26 Aug 2014 09:12:23